

# Methane sources in arctic thermokarst lake sediments on the North Slope of Alaska

P. B. MATHEUS CARNEVALI,<sup>1,2</sup> M. ROHRSEN,<sup>3</sup> M. R. WILLIAMS,<sup>3</sup> A. B. MICHAUD,<sup>4</sup> H. ADAMS,<sup>4</sup> D. BERISFORD,<sup>5</sup> G. D. LOVE,<sup>3</sup> J. C. PRISCU,<sup>4</sup> O. RASSUCHINE,<sup>1,2</sup> K. P. HAND<sup>6</sup> AND A. E. MURRAY<sup>1</sup>

<sup>1</sup>Division of Earth and Ecosystem Sciences, Desert Research Institute, Reno, NV, USA

<sup>2</sup>Department of Biochemistry and Molecular Biology, University of Nevada, Reno, NV, USA

<sup>3</sup>Department of Earth Sciences, University of California, Riverside, CA, USA

<sup>4</sup>Department of Land Resources and Environmental Science, Montana State University, Bozeman, MT, USA

<sup>5</sup>Propulsion, Thermal and Materials Engineering, Jet Propulsion Laboratory, California Institute of Technology, Pasadena, CA, USA

<sup>6</sup>Solar System Exploration, Jet Propulsion Laboratory, California Institute of Technology, Pasadena, CA, USA

## ABSTRACT

The permafrost on the North Slope of Alaska is densely populated by shallow lakes that result from thermokarst erosion. These lakes release methane (CH<sub>4</sub>) derived from a combination of ancient thermogenic pools and contemporary biogenic production. Despite the potential importance of CH<sub>4</sub> as a greenhouse gas, the contribution of biogenic CH<sub>4</sub> production in arctic thermokarst lakes in Alaska is not currently well understood. To further advance our knowledge of CH<sub>4</sub> dynamics in these lakes, we focused our study on (i) the potential for microbial CH<sub>4</sub> production in lake sediments, (ii) the role of sediment geochemistry in controlling biogenic CH<sub>4</sub> production, and (iii) the temperature dependence of this process. Sediment cores were collected from one site in Siqlukaq Lake and two sites in Sukok Lake in late October to early November. Analyses of pore water geochemistry, sedimentary organic matter and lipid biomarkers, stable carbon isotopes, results from CH<sub>4</sub> production experiments, and copy number of a methanogenic pathway-specific gene (*mcrA*) indicated the existence of different sources of CH<sub>4</sub> in each of the lakes chosen for the study. Analysis of this integrated data set revealed that there is biological CH<sub>4</sub> production in Siqlukaq at moderate levels, while the very low levels of CH<sub>4</sub> detected in Sukok had a mixed origin, with little to no biological CH<sub>4</sub> production. Furthermore, methanogenic archaea exhibited temperature-dependent use of *in situ* substrates for methanogenesis, and the amount of CH<sub>4</sub> produced was directly related to the amount of labile organic matter in the sediments. This study constitutes an important first step in better understanding the actual contribution of biogenic CH<sub>4</sub> from thermokarst lakes on the coastal plain of Alaska to the current CH<sub>4</sub> budgets.

Received 16 May 2014; accepted 19 December 2014

Corresponding authors: A. E. Murray. Tel.: +1 775 673 7361; fax: +1 775 673 7635; e-mail: alison.murray@dri.edu and K. P. Hand. Tel.: +1 626 487 5379; fax: +1 818 393 4445; e-mail: kevin.p.hand@jpl.nasa.gov

## INTRODUCTION

Thermokarst lakes, resulting from ground ice melting in permafrost regions (Howard & Prescott, 1973; French, 1976; Kokelj & Jorgenson, 2013), may be the significant

contributors to the global CH<sub>4</sub> budget (Oechel *et al.*, 1993; Phelps *et al.*, 1998; Walter *et al.*, 2007; Schuur *et al.*, 2009). A large proportion of this CH<sub>4</sub> may be derived from ancient thermogenic CH<sub>4</sub> trapped deep within or under the permafrost (referred to as the

'cryosphere cap,' Walter Anthony *et al.*, 2012). However, the large amount of organic matter stored in the thaw layer (talik) between the water column and the permafrost table (Ling & Zhang, 2003; Pedersen *et al.*, 2011; Parsekian *et al.*, 2013), from either interglacial or contemporary photosynthesis, also serves as a significant source of carbon for *in situ* methanogenesis. Identifying and deconvolving the production sources of CH<sub>4</sub> will improve our ability to generate accurate predictions about the changing climate in the Arctic.

The North Slope of Alaska has extensive continuous permafrost (~60–75% ice by volume and ~400 m deep; Sellmann *et al.*, 1975; Hinkel *et al.*, 2003; Jorgenson *et al.*, 2008) and is occupied by thousands of shallow (~2–3 m deep), relic (i.e., drained), and contemporary thermokarst lakes (Hussey & Michelson, 1966; Frohn *et al.*, 2005; Jorgenson & Shur, 2007) that are ice-covered or frozen to the ground for at least 9 months of the year. Northern Alaska lake sediments may be gradually eroded through the lake thaw cycle and preferentially redeposited at the upwind and downwind lake margins (Carson & Hussey, 1962; Hinkel *et al.*, 2003). Relative contributions from allochthonous or autochthonous sources of organic matter have not been well studied in the sediments of this area. Allochthonous organic matter can be transported via fluvial or eolian processes and derive from modern active layer soils or Pleistocene-aged terrigenous organic matter from permafrost (Repenning, 1983). Autochthonous organic matter can be produced by present-day lacustrine autotrophs (Ramlal *et al.*, 1994; Hecky & Hesslein, 1995; Bonilla *et al.*, 2005) and is potentially more labile than allochthonous organic matter.

The coastal plain in the North Slope of Alaska also contains an estimated 53 billion cubic feet of natural gas (Houseknecht *et al.*, 2010). Radiocarbon analyses have indicated that gas seeps in the area may be sourced from the gas reservoirs at depth and/or laterally from thermogenic CH<sub>4</sub> trapped under the permafrost ice cap, rather than from present-day microbial activity within the lake, as is common in Siberia (Walter Anthony *et al.*, 2012). A distinction between microbial and thermogenic CH<sub>4</sub> can be made by combining isotopic ratios (e.g.,  $\delta^{13}\text{C}_{\text{CH}_4}$ ,  $\delta^{13}\text{C}_{\text{CO}_2}$ , and  $\delta\text{D-CH}_4$ ) and C2–C4 hydrocarbon ratios (Whiticar, 1999). Microbial CH<sub>4</sub> production, in which  $\delta^{13}\text{C}$  ranges between –110 and –50‰ (Quay *et al.*, 1988; Whiticar, 1999), results from anaerobic decomposition of organic matter in sediments. Thermogenic CH<sub>4</sub> has a range between –52 and –20‰ (Whiticar, 1999; Judd, 2000; Kvenvolden & Rogers, 2005), and it is generated at subsurface depths between 1 and 4 km by decomposition of residual organic matter under high pressure and temperature, during coal formation or thermal alteration of oil (Judd, 2000).  $\delta^{13}\text{C}_{\text{CH}_4}$  signatures at the boundary between biogenic and thermogenic CH<sub>4</sub> could result from mixed

sources, including CH<sub>4</sub> oxidation, advanced stage of parent organic matter decomposition, contributions from different methanogenic pathways, or a combination of thermogenic and biogenic signatures (Whiticar, 1999). Lastly, abiogenic CH<sub>4</sub> originates in the mantle, and it has a  $\delta^{13}\text{C}$  between –45 and –5‰ (Judd, 2000).

Our study focused on biological CH<sub>4</sub> production in two Alaskan thermokarst lakes. Specifically, we examined the following: (i) *in situ* CH<sub>4</sub> concentrations and carbon isotope compositions of CH<sub>4</sub> in sediments; (ii) temperature response of methanogenesis at natural substrate levels; (iii) archaeol lipid biomarkers (archaeol) and the methyl coenzyme reductase alpha subunit (*mcrA*) gene, which is a key enzyme in the pathway for methanogenesis; and (iv) description of the substrates available for methanogenesis.

## METHODS

### Sampling sites

Siqlukaq Lake (Siq) and Sukok Lake (Suk), two arctic thermokarst lakes near the town of Barrow, Alaska (Fig. 1), were sampled during late October to early November field campaigns. Two sites were sampled at Sukok: one near an active, submerged natural gas seep (Sukok Seep – SukS), and another about 1 km southwest from the seep site (Sukok B site – SukB), to determine the effects of localized CH<sub>4</sub> flux on biological CH<sub>4</sub> production within these

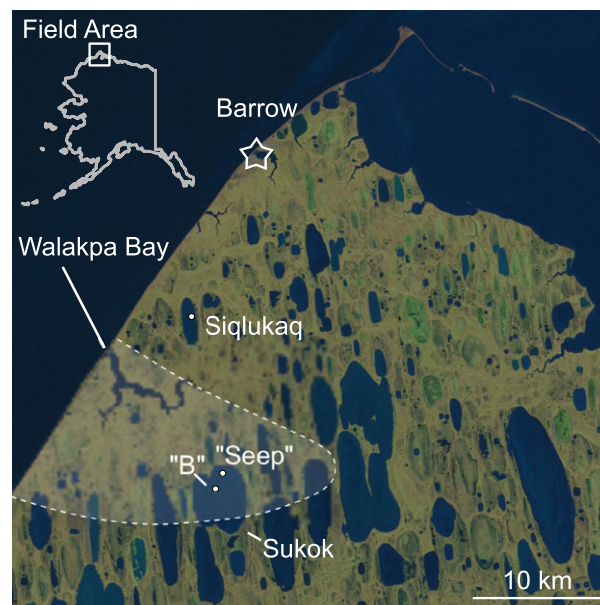


**Fig. 1** Landsat 7 image of the Arctic Coastal Plane near Barrow, AK (L7 ETM+SLC-on, 31 August 2000). Shaded field and hatched lines approximate subsurface boundaries of the Walakpa Gas Field (Glenn & Allen, 1992). Dots indicate sites described in the main text: Siqlukaq (Siq) and the two Sukok Lake sites are 'Seep' proximal to an active, ebullient gas seep (SukS), and 'B' distal from the area of active CH<sub>4</sub> seepage (SukB).

sediments. A total of 16 sediment cores were recovered for various geochemical and biological analyses over the course of four field campaigns spanning 4 years (Table 1). Sediments in both lakes lack well-defined sedimentological features, such as laminations, and the lakes possess taliks of at least 1.1 m depth (the maximum sediment thickness penetrated in coring).

Suk is located ~29 km south of Barrow and 12.7 km east-southeast of the mouth of Walakpa Bay, in the Walakpa gas field, a natural gas field approximately 600 m deep (the permafrost base nearby the lake is ~280 m; Glenn & Allen, 1992). An east-southeast trending fault occurs in the subsurface north of Sukok; however, no such feature is identified beneath the lake itself (Glenn & Allen, 1992). Openings in the ice cover resulting from active CH<sub>4</sub> ebullition in the lake were observed in April 2010 and the late October-early November 2010-2013 field campaigns. Satellite imagery indicates that Suk consists of at least three coalesced thermokarst lakes and lies within a portion of the arctic coastal plain that has seen repeated thermokarst episodes (Fig. 1). Suk is approximately 4.2 km wide and 5.5 km long (not including the slightly adjoined southern basin). At the time of sampling, total water depth for Suk was ~0.80-1.35 m, with ~0.10-0.25 m of ice, and lake water temperatures were relatively uniform with depth between 0.7 and 1.3 °C, as determined with a portable Orion 5 star multimeter (Thermo Scientific, Waltham, MA, USA).

Siq, located 6.6 km east-northeast of the mouth of Walakpa Bay, outside of the gas field, has no visible open holes in winter lake ice due to gas ebullition. Satellite photography shows that Siq likely drains into Walakpa Bay at high stand and shows evidence of previously higher lake levels, but a less complex hydrologic history than that of Suk (Fig. 1). Siq is smaller and more elongated than Suk, measuring approximately 1.0 km wide by 3.8 km long. During the sampling period, Siq was ~1.5-1.6 m deep and had ~0.15-0.25 m of ice, and lake water temperatures between 0.2 and 2.0 °C.

### Sediment geochemistry

Sediment cores were retrieved from all sampling sites using a universal percussion corer (Aquatic Research Instruments), ~10 cm in diameter polycarbonate coring tube, and plug caps on both ends to decrease oxidation. Sediment core lengths ranged between 20 and 110 cm.

#### Oxygen (O<sub>2</sub>) microelectrode profiles

Shallow sediment cores (20 cm) were collected at each sampling site (Siq13, SukB13, and SukS13, Table 1). Overlying water (4.5 cm) was left on top of the sediment to minimize atmospheric O<sub>2</sub> influence on the microprofile in the sediment (Boetius & Damm, 1998). Microelectrode

O<sub>2</sub> profiles were conducted within 30 min of core collection using a Clark-style oxygen microelectrode (Unisense, Aarhus, Denmark) with a tip diameter of 500 µm. These microelectrodes respond in a linear fashion to O<sub>2</sub> concentration (Revsbech, 1989), and a two-point calibration curve was used to standardize the instrument. The microelectrode was attached to a manual micromanipulator and lowered through the water and sediment column at 100-µm increments. Profiling was conducted in a darkened tent which provided a thermal barrier to prevent freezing and to maintain core temperatures (2.7-6.0 °C) during profiling.

Depth-integrated aerobic O<sub>2</sub> consumption (IOC) was calculated using Fick's second law of diffusion assuming zero-order kinetics (Nielsen *et al.*, 1990; Rasmussen & Jørgensen, 1992). The corrected diffusion coefficient ( $D_s$ ) was calculated by adjusting the O<sub>2</sub> diffusion coefficient in freshwater (at sediment temperature during profiling) for porosity and tortuosity, based on measured porosity values and sediment type (Broecker & Peng, 1974; Rasmussen & Jørgensen, 1992).

#### Pore water chemistry

Dissolved gas and chemical gradients in the sediments were determined for deeper cores (50-70 cm) collected from Siq (Siq12-a and Siq12-c) in 2012 and from Suk (SukS13-b, SukS13-c, SukB13-b, and SukB13-d) in 2013 (Table 1). Pore waters were sampled through predrilled holes in the core liners (sealed from the surrounding environment until samples were taken) using Rhizons (Seeberg-Elverfeldt *et al.*, 2005). The ~0.15-µm porous membrane of each Rhizon was conditioned before sampling by rinsing with milli-Q water. Samples were drawn into 10-mL sterile syringes connected to the Rhizons.

Pore water samples for the analysis of low molecular weight organic acids including acetate and formate, and anions SO<sub>4</sub><sup>2-</sup> and NO<sub>3</sub><sup>-</sup>, were collected in 2012 from Siq. Samples were collected (5-mL HDPE bottles), frozen, and then transported to the Biogeochemistry Laboratory at Indiana State University. A Dionex ICS-2000 with an AS11-HC column (Sunnyvale, CA, USA) was utilized to measure the concentration of each compound following Johnson *et al.* (2012) and Baker & Vervier (2004). Due to technical issues, acetate and formate were only measured in the surficial samples at Siq. Samples for the analyses of the anions SO<sub>4</sub><sup>2-</sup> and NO<sub>3</sub><sup>-</sup> collected (15-mL polypropylene tubes) from Suk in 2013 were frozen and then transported to the University of Tennessee, Knoxville. Pore waters were analyzed using a Dionex ICS-2100 RFIC fitted with an ASRS-4 mm suppressor column, an AS18 analytical column, and an AG18 guard column following methods similar to Banihani *et al.* (2009).

Pore water samples for metals analysis collected (15-mL polypropylene tubes) from Siq and Suk were acidified with

**Table 1** Sampling sites, dates, and analyses performed on each core. Cores were labeled using the first three letters to indicate the lake, the next letter to indicate the site (only in the case of Sukkok Lake), followed by the last two digits of the year, and replicate cores indicated by a, b, c, and d

Coordinates (N, W)	Sampling dates	O <sub>2</sub> profile	Pore water chemistry	Total carbon	Lipid biomarkers	<i>mcrA</i> qPCR	[CH <sub>4</sub> ] and $\delta^{13}\text{C}_{\text{CH}_4}$	Porosity	CH <sub>4</sub> production	Sediment texture
<b>Siqluqaq</b>										
71° 10.486'	29-October-2010	-	-	Siq10-a	Siq10-a	-	-	-	-	-
156° 53.891'										
71° 10.481'	22-October-2011	-	-	Siq11-a	Siq11-a	Siq11-a	Siq11-a*	-	Siq11-b	Siq11-b
156° 53.910'										
71° 10.482'	30-October-2012	-	Siq12-a†	-	-	-	Siq12-a	-	-	-
156° 53.900'										
71° 10.457'	02-November-2012	-	Siq12-c†	-	-	-	Siq12-c	-	-	-
156° 54.004'										
71° 10.451'	01-November-2013	Siq13-a	-	-	-	-	-	-	-	-
156° 53.872'										
<b>Sukkok B</b>										
71° 04.006'	24-October-2011	-	-	SukB11-a	SukB11-a	SukB11-a	SukB11-a	-	SukB11-b	SukB11-b
156° 49.841'										
71° 04.006'	02-November-2013	SukB13-a	SukB13-b	-	-	-	SukB13-c	SukB13-c	-	-
156° 49.841'										
71° 03.997'	06-November-2013	-	SukB13-d	-	-	-	-	-	-	-
156° 49.918'										
<b>Sukkok S</b>										
71° 04.455'	27-October-2010	-	-	SukS10-a	SukS10-a	-	-	-	-	-
156° 49.250'										
71° 04.519'	20-October-2011	-	-	SukS11-a	SukS11-a	SukS11-a	SukS11-a	-	SukS11-b	SukS11-b
156° 49.208'										
71° 04.513'	31-October-2013	SukS13-a	SukS13-b	-	-	-	-	-	-	-
156° 49.202'										
71° 04.519'	05-November-2013	-	SukS13-c	-	-	-	SukS13-d	SukS13-d	-	-
156° 49.204'										

\* $\delta^{13}\text{C}_{\text{CO}_2}$  were also analyzed in these cores. †Acetate concentration, formate concentration.

UHP HNO<sub>3</sub> to a final concentration of 1% HNO<sub>3</sub> (vol/vol) in the field and stored at room temperature for <60 days. The 5 mL samples were brought to 10 mL with 1% UHP HNO<sub>3</sub> before analysis. A Thermo Element II high-resolution inductively coupled plasma mass spectrometer with a PFA-ST concentric Teflon nebulizer (ESI, Inc. Portland, OR, USA) and a spray chamber of cyclonic glass (ESI, Inc.) in the Ultratrace Chemistry Laboratory at the Desert Research Institute in Reno, NV, was used to quantify the metals. Low (LR) and medium (MR) resolutions were used as needed for isotopic separations. Standards were made from mixed stock standard from Inorganic Ventures, Inc. (Christiansburg, VA, USA) in a 1% UHP HNO<sub>3</sub> matrix, and all blanks were made of 1% UHP HNO<sub>3</sub>.

### Sediment CH<sub>4</sub>

#### CH<sub>4</sub> concentrations and stable carbon isotope analyses

One sediment core per sampling site was collected in 2011 (Siq11-a, SukB11-a, and SukS11-a) to determine CH<sub>4</sub> concentrations and stable isotope signatures. The cores were sampled on site following Riedinger *et al.* (2010) and Koch *et al.* (2009). Samples were preserved at ~4 °C and analyzed at the University of California Santa Barbara (UCSB), for CH<sub>4</sub> concentration, δ<sup>13</sup>C<sub>CH<sub>4</sub></sub>, and δ<sup>13</sup>C<sub>CO<sub>2</sub></sub>, following methods by Kinnaman *et al.* (2007), with the exceptions that the bottle headspaces were displaced with 1–5 mL degassed water containing NaCl (35 g L<sup>-1</sup>), and 1 mL sample was injected onto a 250-μL sample loop for quantitation. CH<sub>4</sub> concentration (μmoles CH<sub>4</sub> g<sup>-1</sup> sediment dry weight) was estimated from the molar fraction of CH<sub>4</sub> in the headspace using equation 1 from D'hondt *et al.* (2003), excluding the terms for porosity and sediment volume and including sediment dry weight.

To determine inter-annual variability of CH<sub>4</sub> concentrations and C isotopic composition, additional cores were collected from Siq in 2012 (Siq12-a and Siq12c) and from Suk (SukB13-c and SukS13-d) on November 2013. Parallel sediment plugs were collected for porosity analysis within 1.5 cm of samples for CH<sub>4</sub> and CO<sub>2</sub> analysis and were stored at ~4 °C (Riedinger *et al.*, 2010). The approximate ratio of sediment mass to volume in each syringe was obtained by measuring the total volume and wet weight of sediment. Water content was determined using dry weight after heating at 105 °C for 24 h. Porosity was calculated as water volume divided by wet sediment volume.

For comparison, CH<sub>4</sub> concentration was also estimated in μM following equation 1 in D'hondt *et al.* (2003) and using an average porosity from depths sampled in SukB13-c and SukS13-d (data were not available for Siq) and an average sediment volume of 2.7 ± 0.7 mL. Sediment volume was estimated from the average bottle headspace, the known volume of NaCl solution, and the average known volume of the bottles with stoppers.

#### CH<sub>4</sub> production experiment

Samples were obtained for CH<sub>4</sub> production experiments from sediment cores collected in 2011 (Siq11, SukS11, and SukB11) at the same time and within ~15 cm of those for *in situ* CH<sub>4</sub> concentration and stable carbon isotope analysis (Table 1). Sediment cores for these experiments were transported at <4 °C to a cold room, where they were maintained at 2 °C for 1 month. Each core was cut in three sections of approximately equal size, subsampled inside an anaerobic chamber (3–4% H<sub>2</sub>/N<sub>2</sub> atmosphere), and mixed with approximately equal volumes of cold, sterile, anoxic, deionized water by stirring, to eliminate any gas that may have been 'trapped' in the sediments (Kiene & Capone, 1985). Sediment slurries in 10-mL aliquots were distributed among 18 sterile, 125-mL serum bottles (capped with butyl rubber stoppers) per depth. Negative controls with the same water and bottles were also prepared in the anaerobic chamber. The headspace of the bottles was exchanged with ultra-high-purity N<sub>2</sub> for 5 min using a manifold with 0.2-μm filters and sterile needles.

The sediment slurries were incubated upside down at 2 or 10 °C for the duration of the experiment. Time zero samples were collected after 2-h incubation. For all time points, headspace samples were collected with a gas tight syringe (Hamilton, Reno, NV, USA) following vigorous shaking, before and after autoclaving of sediment slurries. Samples were analyzed with a Mini 2 gas chromatograph (GC; Shimadzu, Kyoto, Japan) equipped with a flame ionization detector (FID), a Poropak T column, and the following settings: oven temperature 20 °C, injection port temperature 210 °C, and ultra-high-purity nitrogen as carrier gas at a flow rate of 40 mL min<sup>-1</sup>. The injection volume was 100 μL. Peak area was quantified with a Hewlett-Packard 3390A integrator. CH<sub>4</sub> standards were used for calibration. The headspace of triplicate samples was analyzed every 5–10 days (depending on when CH<sub>4</sub> was first detected), for a period of 25–60 days depending on the lake.

At the end of the experiment, the dry weight of the sediments was determined after drying for 24 h at 105 °C. The CH<sub>4</sub> concentration in the headspace (μmoles CH<sub>4</sub> g<sup>-1</sup> of dry weight) was determined as explained in Section 'CH<sub>4</sub> concentrations and stable carbon isotope analyses'. Additionally, average CH<sub>4</sub> production (accumulation) over time was estimated. Methane production rates were calculated from a linear regression of three consecutive data points. The temperature coefficient (Q<sub>10</sub>) was calculated following Duc *et al.* (2010).

#### Quantitative PCR of the methyl coenzyme reductase alpha subunit gene (*mcrA*)

Sediment subsamples were obtained from the first 30 cm of the 2011 cores Siq11-a, SukS11-a, and SukB11-a (Table 1). Subsamples that were stored at -80 °C were

later transferred to sucrose lysis buffer to preserve the integrity of the nucleic acids (SLB, 40 mM EDTA, 50 mM Tris-HCl, 0.75 M sucrose) prior to nucleic acid extractions. Community genomic DNA from surface sediment subsamples from each lake was extracted using a modified protocol for the power soil DNA isolation kit (MoBio, Carlsbad, CA, USA). Samples in SLB were thawed on ice for 45 min and centrifuged at  $10\,000 \times g$  for 10 min. The supernatant was removed;  $\sim 0.5$  g sediment subsamples (for a total weight of  $\sim 1$  g per sample) were extracted following manufacturer's instructions and later quantified using a standard picogreen assay (Life Technologies, Grand Island, NY, USA).

To quantify *mcrA* gene fragment copy number, quantitative PCR (qPCR) was carried out using the ML primer pair (Luton *et al.*, 2002) and the following conditions:  $1 \times$  SYBR Green PCR master mix,  $0.1 \mu\text{M}$  of each primer, and  $0.1 \mu\text{g} \mu\text{L}^{-1}$  of bovine serum albumin (BSA) in a  $25 \mu\text{L}$  final volume. One microlitre of template DNA from Siq samples was used in 2–4 replicate reactions, and  $4 \mu\text{L}$  of SukS or SukB samples was used in another set of four replicate reactions. A standard curve was prepared using *Methanocaldococcus jannaschii* genomic DNA with  $1 \mu\text{L}$  of 10-fold dilutions covering five orders of magnitude ( $6.4 \times 10^6$  to  $6.4 \times 10^2$  copies of *mcrA* gene assuming 1 copy of *mcrA* per genome), four replicates each. qPCR was performed using an Applied Biosystems 7500 Fast system (Life Technologies) in standard mode and following PCR conditions by Luton *et al.* (2002). PCR efficiency was 75.7%, and amplification of standards was linear ( $r^2 = 0.993$ ) from  $10^2$  to  $10^6$  copies of the template per  $\mu\text{L}$ . *McrA* gene copy numbers were expressed per g of wet sediment and per ng DNA. To confirm amplification specificity, a melt curve analysis was performed immediately after qPCR using standard instrument settings, and agarose gel electrophoresis was used to confirm expected amplicon size.

### Organic carbon and lipid biomarkers analyses

#### *Sediment texture, total carbon, and inorganic carbon content*

Sediment texture was determined following a simple texture analysis chart (Thien, 1979), with the same cores (Siq11-b, SukB11-b, and SukS11-b) used for the  $\text{CH}_4$  production experiment. Total carbon (TC) and total inorganic carbon (TIC) content was determined from five cores: Siq10-a, SukS10-a, Siq11-a, SukS11-a, and SukB11-a. Frozen cores were sectioned every 5 cm to a depth of 30 cm (2011 only) and every 10 cm for the remaining length of each core. These samples were collected into furnace (550 °C, 8 h) glass vials with foil lids that were refrozen ( $-20$  °C) for transportation to the University of California, Riverside. Samples were lyophilized and then

analyzed using an Eltra CS-500 carbon-sulfur analyzer, yielding TC and TIC. Total organic carbon (TOC) was obtained by subtraction.

#### *Lipid biomarker analyses*

Lipid biomarkers were extracted from lyophilized samples obtained from the same cores sampled above using a Microwave Accelerated Reaction System (CEM Corp., Matthews, NC, USA) with 9:1 vol/vol dichloromethane/methanol to yield total lipid extracts (TLEs). One aliquot of each TLE was derivatized with N,O-bis(trimethylsilyl)trifluoroacetamide (BSFTA) in pyridine before gas chromatography-mass spectrometry (GC-MS). A second aliquot of total extract was fractionated via solid-phase extraction columns to yield neutral lipids that were also subjected to GC-MS. Catalytic hydrolysis (HyPy; Love *et al.*, 2005) was applied to an additional aliquot of freeze-dried sediment. HyPy conditions were 5 wt. % molybdenum sulfide catalyst, 150 bar  $\text{H}_2$  flowing at  $5 \text{ L min}^{-1}$ , and programmed temperature ramp of  $100 \text{ }^\circ\text{C min}^{-1}$  to  $250 \text{ }^\circ\text{C}$ , followed by ramping at  $8 \text{ }^\circ\text{C min}^{-1}$  to  $480 \text{ }^\circ\text{C}$ . Gas chromatography-mass spectrometry (GC-MS) analyses of freely extractable and kerogen-bound saturated hydrocarbons, and derivatized total extracts were performed with an Agilent 5973 MSD mass spectrometer interfaced to an Agilent 7890A GC, equipped with a DB-1MS capillary column ( $60 \text{ m} \times 0.32 \text{ mm}$ ,  $0.25\text{-}\mu\text{m}$  film) and run with He as carrier gas. The temperature program for GC-MS full scan and selected ion monitoring was  $60 \text{ }^\circ\text{C}$  (2 min), ramp to  $250 \text{ }^\circ\text{C}$  at  $20 \text{ }^\circ\text{C min}^{-1}$ , to  $325 \text{ }^\circ\text{C}$  at  $2 \text{ }^\circ\text{C min}^{-1}$ , and held at  $325 \text{ }^\circ\text{C}$  for 20 min. Lipid biomarkers were identified by comparison with published mass spectra and retention times and quantified using a d4- $\alpha\alpha\alpha$ -24-ethylcholestane internal standard. Archaeol was quantified using  $m/z$  130 in selected ion monitoring mode with a d14-*para*-terphenyl internal standard ( $m/z$  244) and calculated response factor. The response factor was obtained by the comparison of detector response areas between replicate analyses of known amounts of archaeol and d14-*p*-terphenyl.

## RESULTS

### Sediment geochemistry

#### *Oxygen profiles and depth-integrated aerobic $\text{O}_2$ consumption*

Dissolved  $\text{O}_2$  concentration at the sediment-water interface in freshly collected cores from Siq13, SukB13, and SukS13 was 212.4, 110.0, and  $6.5 \mu\text{mol L}^{-1}$ , respectively (Fig. 2). Oxygen decreased rapidly with depth in all cores, becoming depleted by 1.0, 10.0, and 0.5 mm in the same respective cores. The depth of  $\text{O}_2$  depletion typically coincided with concentration at the sediment-water interface in the Suk cores; cores from Siq did not fit this trend indicating

that O<sub>2</sub> dynamics in Siq were different from those in Suk. Based on the shape of the O<sub>2</sub> depletion profiles, and assuming steady state conditions, average ( $\pm$ SD) rates of metabolic O<sub>2</sub> consumption were estimated to be 503.5–892.9,  $40.8 \pm 14.4$ , and  $72.6 \pm 19.1 \mu\text{mol O}_2 \text{ m}^{-2} \text{ h}^{-1}$  in cores from Siq, SukB, and SukS, respectively.

#### Pore water chemistry

Pore water chemistry from Siq12 sediment cores was generally reproduced in replicate cores. The average concentration of NO<sub>3</sub><sup>-</sup> ( $76.62 \pm 73.18 \mu\text{M}$ ) and SO<sub>4</sub><sup>2-</sup> ( $8.74 \pm 8.47 \mu\text{M}$ ) in the upper 8 cm of the two replica cores was higher than the average concentration of NO<sub>3</sub><sup>-</sup> ( $1.40 \pm 2.51 \mu\text{M}$ ) and SO<sub>4</sub><sup>2-</sup> ( $0.96 \pm 0.70 \mu\text{M}$ ) below 8 cm (Fig. 3A,J). The concentration of total dissolved Fe in both cores was high throughout the depth profile, reaching a maximum ( $854.94 \mu\text{M}$  at 20 cm in Siq12-a) between 12 and 20 cm below the sediment–water interface. Additionally, the concentration of total dissolved Mn in the pore waters was about 44-fold lower than the concentration of total dissolved Fe, but showed a similar depth profile to Fe (Fig. 3D,G).

Overall, the concentration of NO<sub>3</sub><sup>-</sup> and SO<sub>4</sub><sup>2-</sup> in Suk was higher than the concentration of these anions in Siq. Reproducibility between cores at the same site was poor. Two maxima were detected in SukB13-b ( $2.34 \text{ mM}$  at 10 cm and  $745.73 \mu\text{M}$  at 18 cm), but the concentrations were much lower ( $0.00\text{--}27.47 \mu\text{M}$ ) in the rest of the core (sampled to 30 cm), as well as in SukB13-d ( $0.87\text{--}52.58 \mu\text{M}$ ; Fig. 3B). In SukS13-b, increasing NO<sub>3</sub><sup>-</sup> was detected with increasing depth ( $0.00\text{--}126.25 \mu\text{M}$ ), but in SukS13-c, NO<sub>3</sub><sup>-</sup> peaked at 11 cm ( $1.07 \text{ mM}$ ) and then decreased (Fig. 3C). The SO<sub>4</sub><sup>2-</sup> concentration increased with depth in SukB13-b ( $0.00 \mu\text{M}$  at 2 cm to  $751.68 \mu\text{M}$  at 30 cm), and in SukB13-d, there was an average of

$275.27 \pm 112.74 \mu\text{M}$  throughout the core (sampled to 17 cm) with two maxima of  $\sim 450 \mu\text{M}$  (at 5 and 11 cm; Fig. 3K). The SO<sub>4</sub><sup>2-</sup> concentration mostly increased with depth in the first  $\sim 20$  cm ( $0.00\text{--}329.29 \mu\text{M}$ ) of SukS13-b. A similar pattern was observed in SukS13-c down to  $\sim 17$  cm ( $0.00\text{--}296.42 \mu\text{M}$ ; Fig. 3L).

Depth profiles of dissolved Fe and Mn in SukB13 (Fig. 3E,H) were somewhat similar to Siq12. The concentration of dissolved Fe in SukB increased by 300-fold from 1 cm below the surface to 12 cm below the surface and then decreased with depth; the concentration of dissolved Mn was relatively constant throughout the profile in SukB. The concentration of these metals throughout the sediment profile in SukS (Fig. 3F,I) showed a lack of a curve and was lower than in Siq (dissolved Fe  $\sim$  eightfold and Mn  $\sim$  threefold) and SukB (dissolved Fe  $\sim$  fivefold and Mn  $\sim$  twofold).

#### CH<sub>4</sub> concentrations and stable carbon isotope analyses

##### *In situ* CH<sub>4</sub> concentration and stable carbon isotopes

Average ( $\pm$ SD) CH<sub>4</sub> concentration was orders of magnitude higher in the upper intervals from Siq ( $2.18 \pm 0.24 \mu\text{moles CH}_4 \text{ g}^{-1}$  dry sediment) than in SukB ( $3.12 \pm 2.30 \times 10^{-4} \mu\text{moles CH}_4 \text{ g}^{-1}$  dry sediment) and SukS ( $3.21 \pm 1.44 \times 10^{-3} \mu\text{moles CH}_4 \text{ g}^{-1}$  dry sediment; Fig 4A). CH<sub>4</sub> concentration decreased precipitously with depth in Siq sediments, from  $0.84 \mu\text{moles CH}_4 \text{ g}^{-1}$  dry sediment at  $\sim 38$  cm to  $0.02 \mu\text{moles CH}_4 \text{ g}^{-1}$  sediment at 88 cm. Conversely, CH<sub>4</sub> concentration remained relatively constant throughout the SukB sediment profile ( $7.00 \pm 4.10 \times 10^{-4} \mu\text{moles CH}_4 \text{ g}^{-1}$  sediment), while CH<sub>4</sub> concentration increased with depth in the SukS sediments, with the highest amount of CH<sub>4</sub> observed at 75 cm ( $0.11 \mu\text{moles CH}_4 \text{ g}^{-1}$  dry sediment). The CH<sub>4</sub> level detected in

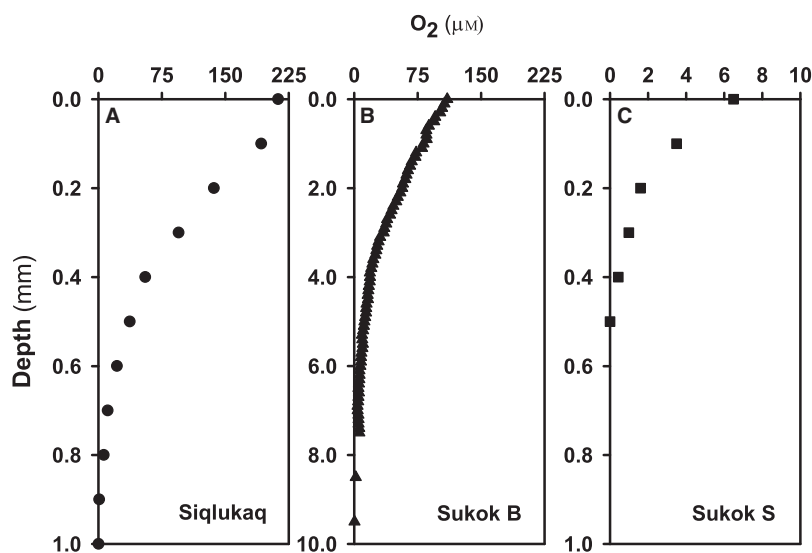
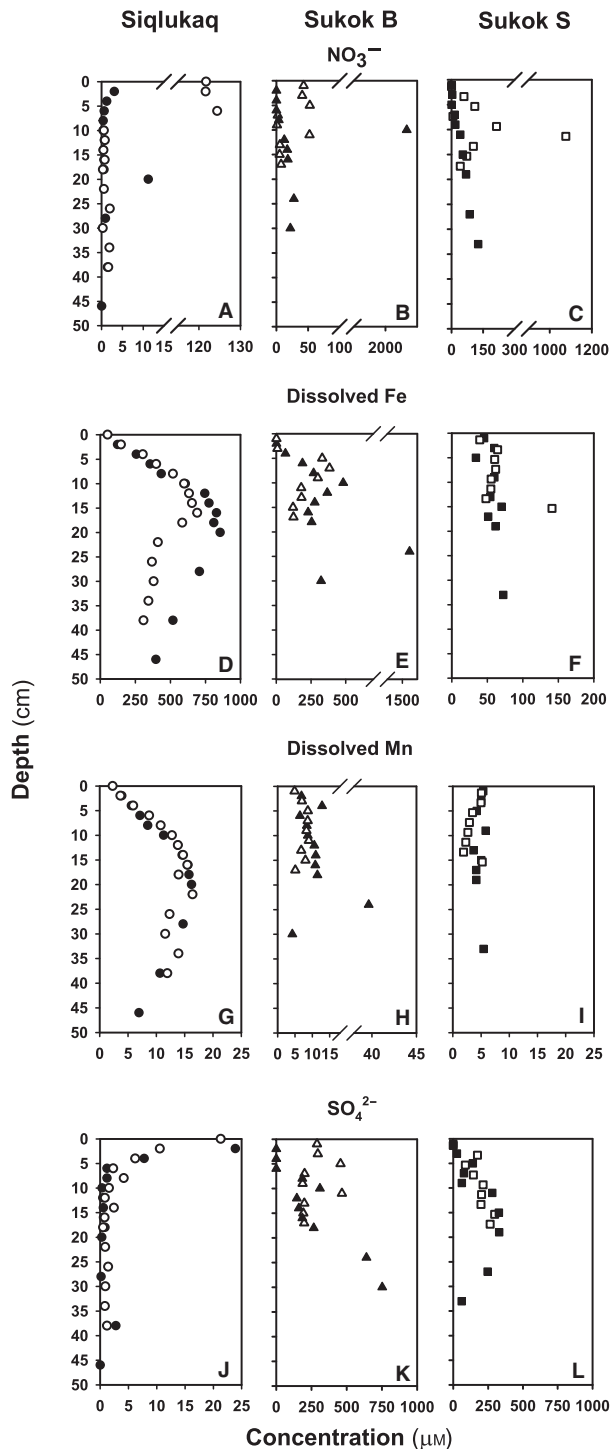


Fig. 2 Oxygen microprofiles measured at 100  $\mu\text{m}$  resolution. (A) Siq13-a, (B) SukB13-a, (C) SukS13-a.



**Fig. 3** Pore water chemistry profiles from replicate sediment cores. (A, D, G, J) Siqlukaq Lake: Siq12-a: black, Siq12-c: white. (B, E, H, K) Sukok site distal to the seep: SukB13-b: black, SukB13-d: white. (C, F, I, L) Sukok Lake, seep site: SukS13-b: black, SukS13-c: white. Note different scales on different axes.

the deepest interval of SukS core was 2 orders of magnitude higher than the amount of CH<sub>4</sub> detected at a similar depth in SukB.

Methane from Siq sediments was more <sup>13</sup>C-depleted than in SukS sediments (Fig. 4B). The most negative δ<sup>13</sup>C<sub>CH<sub>4</sub></sub> values (−76.7 to −79.2 ± 0.2‰) were detected in Siq surface sediment, between 8 and 38 cm. However, the signal became less depleted in <sup>13</sup>C at 58 cm (−64.3 ± 1.6‰), and even less depleted at 88 cm (−43.3 ± 6‰). The δ<sup>13</sup>C<sub>CH<sub>4</sub></sub> values in SukS sediments were less depleted at 35 cm (−55.5 ± 1.4‰) and at 55 cm (−47.3 ± 0.2‰) than those for Siq. The least depleted δ<sup>13</sup>C<sub>CH<sub>4</sub></sub> value in SukS was observed at 75 cm (−43.4 ± 0.2‰). The surface CH<sub>4</sub> concentrations for SukS sediments along with the entire depth profile in SukB were insufficient for the analysis of isotopes.

*CH<sub>4</sub> production experiment*

Biological CH<sub>4</sub> production was observed in sediments from Siq11 at both temperatures (2 and 10 °C), and the upper sediments from SukB11 at 10 °C (Fig. 5). The highest amount of CH<sub>4</sub> produced was 7.4 ± 1.2 µmoles

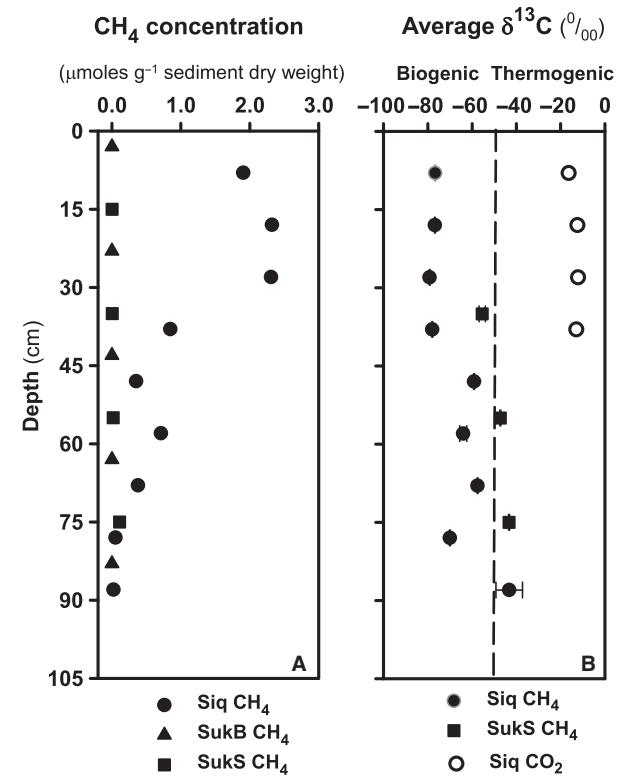


**Fig. 4** Methane concentration, δ<sup>13</sup>C<sub>CH<sub>4</sub></sub> and δ<sup>13</sup>C<sub>CO<sub>2</sub></sub> in arctic thermokarst lakes. (A) CH<sub>4</sub> concentration per gram of dry sediment (Siq11-a, SukB11-a, and SukS11-a). (B) δ<sup>13</sup>C<sub>CH<sub>4</sub></sub> (Siq11-a and SukS11-a) and δ<sup>13</sup>C<sub>CO<sub>2</sub></sub> (Siq11-a) in pore waters. The approximate boundary between biogenic and thermogenic CH<sub>4</sub> (Whiticar, 1999) is indicated with a dashed line for visual convenience. The error for the average CH<sub>4</sub> concentration (analytical replicates) was ±2%. The error for the average δ<sup>13</sup>C<sub>CH<sub>4</sub></sub> (analytical replicates) was ±0.2‰, except at 58 cm (±1.6‰) and 88 cm (~±6.0‰) in Siq, and at 55 cm (±1.4‰) in SukS. For comparison with other data sets, CH<sub>4</sub> concentration in pore waters as µM was estimated in Section 'Implications for CH<sub>4</sub> production from permafrost in the North American Arctic' (main text).

CH<sub>4</sub> g<sup>-1</sup>dry weight ( $n = 3$ ) in the 2- to 20-cm interval of Siq sediments at 10 °C, and  $3.7 \pm 0.0$   $\mu\text{moles CH}_4$  g<sup>-1</sup>dry weight ( $n = 2$ ) at 2 °C after 25 days of incubation (Fig. 5A). The next deeper interval of Siq sediment (26–47 cm) produced  $0.9 \pm 0.2$   $\mu\text{moles CH}_4$  g<sup>-1</sup>dry weight ( $n = 6$ ) at 10 °C and  $0.2 \pm 0.0$   $\mu\text{moles CH}_4$  g<sup>-1</sup>dry weight ( $n = 6$ ) at 2 °C (Fig. 5B). CH<sub>4</sub> production from the 2- to 30-cm SukB-11 sediment interval was not detected until day 10 of incubation at 10 °C. After 50 days of incubation,  $0.3 \pm 0.1$   $\mu\text{moles CH}_4$  g<sup>-1</sup>dry weight ( $n = 6$ ) were produced at 10 °C and  $<0.1$   $\mu\text{moles CH}_4$  g<sup>-1</sup>dry weight ( $n = 6$ ) were produced at 2 °C in this SukB upper interval (Fig. 5D).

Upper Siq and SukB sediments produced more CH<sub>4</sub> than any other interval of sediment sampled. CH<sub>4</sub> production  $<0.1$   $\mu\text{moles CH}_4$  g<sup>-1</sup>dry weight was observed in the deepest interval from Siq (49–76 cm; Fig. 5C), and no CH<sub>4</sub> production was observed in the deeper intervals from SukB (34–62 and 64–90 cm) during the incubation period (Fig. 5E,F). Furthermore, no CH<sub>4</sub> production was observed from the SukS sediments, although very small amounts of CH<sub>4</sub> were detected at all depths sampled.

Temperature had a distinct influence on the rate of CH<sub>4</sub> production (obtained as the slope of a linear regression of three consecutive data points). CH<sub>4</sub> was produced at a rate of  $2.2$   $\mu\text{moles CH}_4$  day<sup>-1</sup> g<sup>-1</sup> dry weight at 10 °C and at a rate of  $0.8$   $\mu\text{moles CH}_4$  day<sup>-1</sup> g<sup>-1</sup> dry weight at 2 °C in the upper Siq sediments. In the next deeper interval of Siq sediment, CH<sub>4</sub> was produced at a much lower rate:  $0.3$   $\mu\text{moles CH}_4$  day<sup>-1</sup> g<sup>-1</sup> dry weight at 10 °C and  $<0.1$   $\mu\text{moles CH}_4$  day<sup>-1</sup> g<sup>-1</sup> dry weight at 2 °C. The temperature coefficient ( $Q_{10}$ ) in Siq was 3.7 for the upper sediment interval and 9.5 for the next interval down indicating different metabolic responses of the microbial community through the sediment core. The rate of CH<sub>4</sub> production in the upper sediments of SukB could only be estimated at 10 °C ( $0.9$   $\mu\text{moles CH}_4$  day<sup>-1</sup> g<sup>-1</sup>dry weight), given that CH<sub>4</sub> did not show a linear increase over time at 2 °C; hence, no  $Q_{10}$  value was computed.

### Proxies for methanogen abundance

The *mcrA* gene was detected in the surface sediments from the three sites by qPCR amplification, but only Siq11 gene

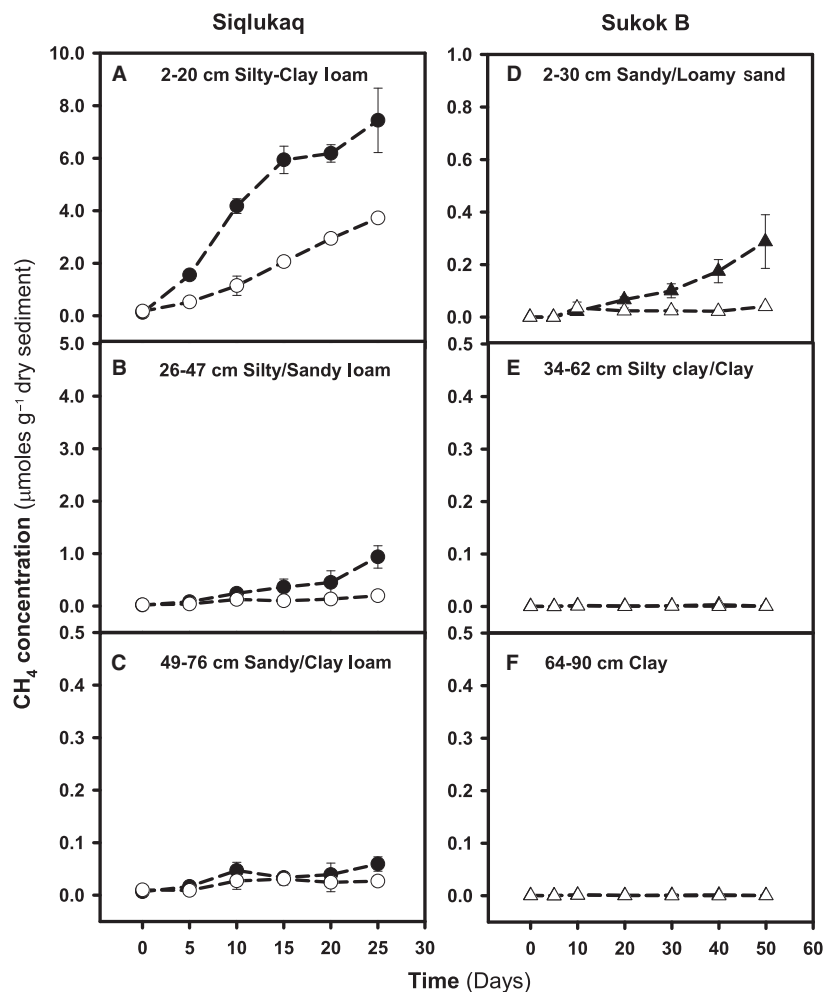


**Fig. 5** CH<sub>4</sub> production from sediment incubations at two temperatures using *in situ* organic matter. CH<sub>4</sub> production at 10 °C (filled symbols) and at 2 °C (open symbols) at three different depths. Siq11-b (A) 2–20 cm, (B) 26–47, and (C) 49–76 cm. SukB11-b (D) 2–30 cm, (E) 34–62 cm, and (F) 64–90 cm. Note the different scales. CH<sub>4</sub> production was an average of 2–6 replicate samples (see Methods). Soil texture from the upper and lower layer of each sediment depth is described in each panel. CH<sub>4</sub> was detected in some incubations from SukS, but no pattern of CH<sub>4</sub> production was observed.

copy numbers were at or above a conservative limit of detection that was established for this assay (100 copies *mcrA*  $\mu\text{L}^{-1}$ ). The highest *mcrA* gene copy number detected was  $1.9 \times 10^4$  *mcrA* copies  $\text{g}^{-1}$  sediment ( $5.4 \times 10^2$  *mcrA* copies  $\text{ng}^{-1}$  DNA) for Siq samples between ~14 and 15 cm below the surface, while the copy number between ~6 and 7 cm was  $6.4 \times 10^3$  *mcrA* copies  $\text{g}^{-1}$  sediment ( $1.3 \times 10^2$  *mcrA* copies  $\text{ng}^{-1}$  DNA), and between 23 and 24 cm was  $5.0 \times 10^3$  *mcrA* copies  $\text{g}^{-1}$  sediment ( $4.7 \times 10^2$  *mcrA* copies  $\text{ng}^{-1}$  DNA).

Archaeol was highest in Siq where two maxima were encountered: 45 and 37  $\mu\text{g g}^{-1}$  sediment at ~12.5 and ~17.5 cm, but was lower outside these intervals (Fig. 6B). Absolute archaeol concentration was greater in the distal seep site, SukB, beginning at 0.1  $\mu\text{g g}^{-1}$  sediment at 7.0 cm, reaching a maximum of 1.4  $\mu\text{g g}^{-1}$  sediment at ~26.5 cm, and then below detection for the lowermost portion of the studied samples. In the SukS11 core, the absolute archaeol concentration was slightly elevated in the upper ~23.5 cm but consistently low ( $\leq 0.07$   $\mu\text{g g}^{-1}$  sediment) throughout the entire 1-m core (2–3 orders of magnitude lower than at Siq and SukB). The archaeol-to-*n*-C<sub>31</sub> ratio (Fig. 6C) was consistently higher in Siq (average  $0.10 \pm 0.05$ ) and SukB (average  $0.08 \pm 0.06$ ) than in the SukS site ( $0.01 \pm 0.01$ ).

#### Sediment properties, organic matter content, and composition

Total organic carbon (TOC) measurements varied widely among and within cores analyzed at the three sites (Fig. 6A). TOC was highest in the upper 40 cm of Siq11 sediment (avg. 14.9 wt. %) and then decreased to an average of 2.1 wt. % at depths >40 cm below the

sediment–water interface. The Siq11 sediment core had an overall average of  $7.2 \pm 2.9$  wt. % TOC. SukB11 exhibited relatively low and consistent carbon contents down core (overall average  $1.9 \pm 3.7$  wt. %), with the exception of a high TOC interval around 23-cm sediment depth (12.9 wt. %). Excluding this interval, the SukB11 core had an average of  $0.9 \pm 0.5$  wt. % TOC. SukS sediments contained the lowest amounts of organic carbon, averaging  $0.5 \pm 0.3$  wt. % over the entire SukS11 sediment core. Sediment TOC profiles from the 2011 samples reported here were consistent with those from a similar sample set collected in 2010 at the same locations (Table S2). Sediment texture analyses of 2011 sediment cores indicated that SukS and Siq have similar grain size profiles, with a dominance of clay and silt (90–95%) in the upper portion of the core, and 60–80% sand in the lower portions. SukB has the opposite profile, with >70% sand in the uppermost portion and 90% silt and clay in the remainder of the core. SukB sediments contained carbonate, which was most likely detrital in origin.

Organic matter sources and composition were evaluated through analysis of saturated hydrocarbons, BSTFA-derivatized TLEs, and catalytic hydrolysis products (functionalized free- and kerogen-bound lipids that have been converted to hydrocarbons). The proportions and amounts of these compounds differed from site to site and with depth at a given site (Tables S2 and S3). Both the extractable and the kerogen-bound hydrocarbons in Siq10 sediments were dominated by intermediate chain length *n*-alkanes. The most abundant *n*-alkane in free hydrocarbons was *n*-C<sub>23</sub> and in the kerogen-bound fraction was *n*-C<sub>24</sub>. The proportion of *n*-alkanes derived from aquatic plants ( $P_{\text{aq}}$  values, average 0.77 for the free hydrocarbons) was consistent with this intermediate chain length. These

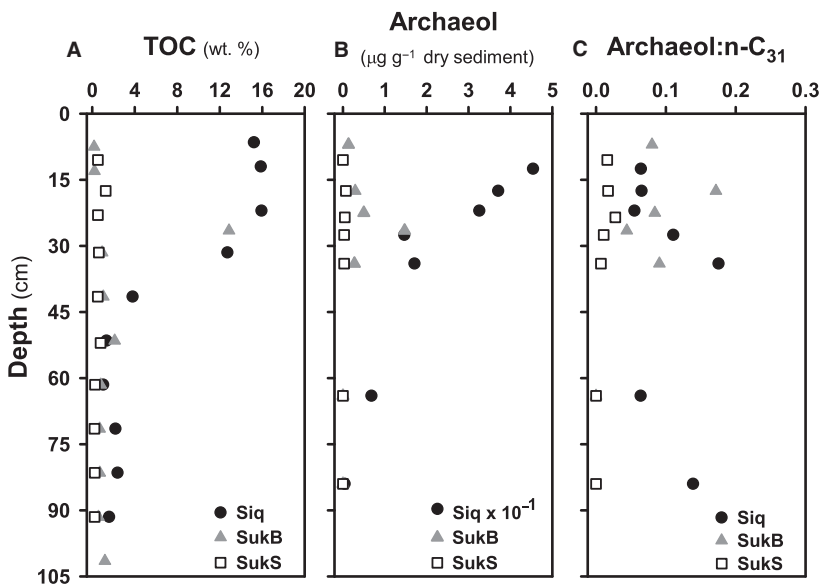


**Fig. 6** October 2011 sediment depth profiles of (A) total organic carbon, (B) archaeol concentration, and (C) archaeol-to-*n*-C<sub>31</sub> ratios. Note that Siq archaeol values are plotted one order of magnitude lower than detected in order to show the variation in the low SukB and SukS values.

samples also contained low short-to-long *n*-alkane ratios and relatively low sterane-to-hopane ratios (free sterane to hopane average 0.03, kerogen-bound sterane to hopane average 2.27). SukS10 organic matter showed a pronounced difference between free hydrocarbons and kerogen-bound hydrocarbons. The most abundant *n*-alkane in the free fraction was *n*-C<sub>31</sub>, but the most abundant *n*-alkane in the bound fraction was *n*-C<sub>16</sub>. The short-to-long *n*-alkane ratio average was 0.02 in the free fraction, and the short-to-long *n*-alkane ratio average in the bound fraction was 7.35. Free *n*-alkanes also had lower  $P_{aq}$  values (average 0.18) in this lake. Carbon preference indices (CPI) for both lakes showed strong odd-over-even predominance in free *n*-alkanes (from decarboxylation of free fatty acids) and even-over-odd in bound *n*-alkanes (from reduction of functionalized lipids).

## DISCUSSION

Methane emissions have received extensive attention in numerous environments (Wagner *et al.*, 2007; Liu *et al.*, 2013; Negandhi *et al.*, 2013), where as much as 80–90% of the atmospheric CH<sub>4</sub> is microbially derived (Whiticar, 1999). Furthermore, atmospheric CH<sub>4</sub> is a potent greenhouse gas that is currently rising (Hoehler & Alperin, 2014). Considering that the Arctic is highly sensitive to climate change (Kittel *et al.*, 2011), accurate estimates of CH<sub>4</sub> emissions are of the utmost importance for the global CH<sub>4</sub> budget. Methane has also been recognized as a bio-signature for life beyond Earth (Tazaz *et al.*, 2013). In this section, we discuss the implications of our findings for North American Arctic CH<sub>4</sub> budgets.

### CH<sub>4</sub> sources and sediment biogeochemistry in Siqukuaq Lake

#### Sediment CH<sub>4</sub> profiles

Detection of CH<sub>4</sub> (highest between 8 and 18 cm below the surface) in Siqukuaq was consistent with rapid O<sub>2</sub> depletion (~1 mm, Fig. 2) and pore water biogeochemistry (Fig. 3). The O<sub>2</sub> concentration in the water–sediment interface was within the range of concentrations detected in other shallow arctic lakes (Whalen *et al.*, 2013), but O<sub>2</sub> was depleted in Siqukuaq at a shallower depth. High amounts of surficial TOC (Fig. 6) in combination with a silty clay loam suggested that Siqukuaq sediments would become anoxic at shallow sediment depths. In fact, within the first 1 mm in the sediment profile, O<sub>2</sub> was consumed at a rate higher than that computed in the other sediment cores we studied. This rate is at the low end of those observed in a eutrophic lake (Lake Zug, Switzerland; Maerki *et al.*, 2009), and it is similar to the rate measured in a meso-eutrophic lake (Lake Vechten, The Netherlands; Sweerts *et al.*, 1991). Moreover, SO<sub>4</sub><sup>2-</sup> and NO<sub>3</sub><sup>-</sup> were consumed within the first

10 cm below the sediment–water interface, while dissolved Fe and Mn were chemically reduced, indicating thermodynamic conditions favorable for methanogenesis deeper in the profile. At depths >48 cm, CH<sub>4</sub> concentration decreased in concert with TOC values. Overall, a positive correlation was found between the *in situ* CH<sub>4</sub> concentration and the TOC content in the sediments ( $r^2 = 0.80$ ,  $P = 0.008$ ), partly explaining the decrease in biological CH<sub>4</sub> production with depth.

#### $\delta^{13}C_{CH_4}$

The stable isotope signature of C in CH<sub>4</sub> ( $\delta^{13}C_{CH_4}$ ) from Siqukuaq sediment suggested a biogenic source (Figs 4 and S2). The most depleted  $\delta^{13}C_{CH_4}$  values ( $-79.2$  to  $-57.6 \pm 0.2\%$ ) fell within the range of  $\delta^{13}C_{CH_4}$  values recorded in the literature for biogenic CH<sub>4</sub> production in other arctic studies (Quay *et al.*, 1988; Walter *et al.*, 2008). Only the deepest sediment layer (~88 cm) in Siqukuaq showed a borderline thermogenic (c.f. Walter Anthony *et al.*, 2012) signal. At this depth, however, substrate depletion due to extensive organic matter decomposition (Pedersen *et al.*, 2011) could result in biogenic CH<sub>4</sub> with heavier  $\delta^{13}C_{CH_4}$  values (Whiticar, 1999).

Biological CH<sub>4</sub> production pathways may be inferred by estimating the isotope separation factor ( $\epsilon_C$ ) between  $\delta^{13}C_{CO_2}$  and  $\delta^{13}C_{CH_4}$  and the apparent C fractionation factor ( $\alpha_C$ ) (Whiticar, 1999). For the upper 38 cm of Siqukuaq sediments, we calculated  $\epsilon_C$  between 60.4 and 67.1 and  $\alpha_C$  between 1.065 and 1.073. This corresponds to CH<sub>4</sub> production by CO<sub>2</sub> reduction (Whiticar, 1999) and is in accordance with the values observed by Walter *et al.* (2008) for ebullient CH<sub>4</sub> sources in Siberian lakes. Alternative pathways, such as acetate fermentation, have been found to occur in freshwater sediments that are rich in organic carbon. Although acetate was present in the first few centimeters of Siqukuaq sediment (0.3–0.6  $\mu$ M), it is possible that other forms of anaerobic respiration outcompeted methanogenesis in the use of acetate, leaving CO<sub>2</sub> reduction as the dominant pathway. For instance, the similarity between the dissolved Fe (Fig. 3D) and CH<sub>4</sub> (Fig. 4A) profiles is not currently understood in these lakes, though could be explained by a syntrophic relationship between iron-reducing bacteria and methanogens (Zhou *et al.*, 2014), in which iron-reducing bacteria oxidize acetate to CO<sub>2</sub>, and the CO<sub>2</sub> is reduced by methanogenic archaea to CH<sub>4</sub> (via the hydrogenotrophic pathway). Despite the little we know about iron reduction in the sediments of these lakes, this process has been connected to ecosystem respiration in drained lake basins on the coastal plain of Alaska (Lipson *et al.*, 2013).

#### CH<sub>4</sub> production

Methane was biologically produced from organic matter present in the first ~47 cm of Siqukuaq11 sediment at 2 °C and

at 10 °C. Coincidentally, the amounts of CH<sub>4</sub> produced at 2 °C were similar to pore water CH<sub>4</sub> levels, indicating that CH<sub>4</sub> present in the sediments was most likely derived from *in situ*, present-day methanogenesis. The rate of CH<sub>4</sub> production at 10 °C in the upper sediments of Siq was in the range of the CH<sub>4</sub> production rates reported for the 0.4–9.0 cm sediment depth of three shallow (4.1–6.7 m) lakes in the Arctic Foothills region of Alaska (Bretz & Whalen, 2014).

These results also suggest that CH<sub>4</sub> was produced in a temperature-dependent fashion. This kind of temperature dependence is expected for biological reactions where enzymes are involved (Hochachka & Somero, 1973) and corroborates the temperature dependence of methanogenesis at the microbial community level recently shown by Yvon-Durocher *et al.* (2014). As observed in surface (2–20 cm) Siq sediment, a 10 °C temperature rise can be correlated to a 2.5- to 3.5-fold increase in CH<sub>4</sub> production (Conrad & Schutz, 1988); however, the threefold increase in the rate of CH<sub>4</sub> production in the next deeper (26–47 cm) Siq interval supports the idea that decomposing structurally complex, aromatic molecules requires higher activation energies, causing enzymatic reactions to be more sensitive to temperature (Mikan *et al.*, 2002; Davidson & Janssens, 2006). Below the methanogenic zone in Siq sediment, older, more recalcitrant organic matter may be found.

## CH<sub>4</sub> sources and sediment biogeochemistry in Sukok Lake

### Sediment CH<sub>4</sub> profiles

CH<sub>4</sub> was not retained in the sediments of Sukok Lake. The low CH<sub>4</sub> concentrations in both SukB and SukS sediments (Fig. 4) were surprising, considering the proximity of the SukS sediments to an ebullient gas seep (Fig. 1). SukS sediments transitioned from silty clay at the upper intervals, to a combination of sandy clay loam and loamy sand in the deeper intervals, perhaps reflecting current- or ebullition-induced winnowing that facilitated CH<sub>4</sub> channeling through the seep. Additionally, lower TOC contents in Suk compared to Siq (by a factor of ~4) may have indirectly affected O<sub>2</sub> levels in the sediments, supporting lower O<sub>2</sub> consumption rates in SukB and in SukS vs. Siq. TOC concentration was slightly higher in SukS than in SukB, and O<sub>2</sub> concentration was lower at the SukS water–sediment interface, but comparable in magnitude to another lake in the Arctic Foothills region (Bretz & Whalen, 2014). The lower TOC content at both Suk sites may also explain the higher concentrations of alternative electron acceptors (NO<sub>3</sub><sup>-</sup> and SO<sub>4</sub><sup>2-</sup>) in the sediments of this lake and establishes the conditions for other biogeochemical transformations to take place in the upper layers of SukB and SukS (i.e., anaerobic methane oxidation).

### δ<sup>13</sup>C<sub>CH4</sub>

Physical mixing of CH<sub>4</sub> from different sources (e.g., microbial and thermogenic) could explain the ‘transitional’ isotope signature observed in SukS. The primary source of CH<sub>4</sub> in the deeper sediment layers was consistent with thermogenic CH<sub>4</sub>, although there may also be some biological CH<sub>4</sub> production in discrete layers of these sediments. Considering that Sukok Lake is located in a gas field and that the sample from SukS was collected nearby an active CH<sub>4</sub> seep, a thermogenic CH<sub>4</sub> signal is plausible. Additional measures of C2–C4 hydrocarbon ratios or δD-CH<sub>4</sub> could be used to further substantiate this observation. Also, methanogenesis could be thermodynamically constrained by high CH<sub>4</sub> partial pressures (like the ones observed at the nearby CH<sub>4</sub> seep) in combination with low concentrations of methanogenic substrates (Chong *et al.*, 2002) or by high redox potentials. Data from the CH<sub>4</sub> production experiment with SukS samples however ruled out the possibility of thermodynamic inhibition imposed by CH<sub>4</sub> itself. Note that the δ<sup>13</sup>C<sub>CH4</sub> for SukB samples could not be determined due to insufficient CH<sub>4</sub> levels.

### CH<sub>4</sub> production

Biological CH<sub>4</sub> production was not observed from any SukS11 interval at 2 or 10 °C, which is consistent with the isotopically heavy δ<sup>13</sup>C<sub>CH4</sub> in SukS11. However, CH<sub>4</sub> production at 10 °C was detected in the upper SukB11 sediments at a rate 23-fold lower than Siq11. Temperature had a weaker influence on CH<sub>4</sub> production in Suk than in Siq. According to Davidson & Janssens (2006), when substrate is abundant, temperature increases affect the maximum reaction rate ( $V_{max}$ ), but under substrate-limiting conditions, the substrate concentration at which the reaction rate equals  $V_{max} [2 (K_m)]^{-1}$  also increases with temperature, leading to a lower apparent temperature dependence. Therefore, the lag phase of CH<sub>4</sub> production observed in SukB surface sediments may be consistent with the observation that organic matter in Suk has a higher vascular plant input and thus may not only be less abundant, but also less labile than in Siq.

The fact that there was more TOC in the surface sediments of SukS than in SukB but there was no CH<sub>4</sub> production in SukS at 10 °C indicates that biological CH<sub>4</sub> production in SukS sediments may be subject to other environmental constraints. Alternatively, longer incubation times or substrate additions could lead to CH<sub>4</sub> production from SukS, as reported in other ecosystems (e.g., Tibetan plateau lakes; Liu *et al.*, 2013).

## Proxies for methanogen abundance as a control on CH<sub>4</sub> concentration in thermokarst lake sediments

Copy numbers of the *mcrA* gene in lake sediments were used to study the relationship between methanogen

biomass and CH<sub>4</sub> concentration in sediment pore waters (Colwell *et al.*, 2008; Freitag & Prosser, 2009; Liu *et al.*, 2011). Assuming the presence of 1 copy of *mcrA* gene per genome of methanogenic archaea, the copy number of the *mcrA* gene may be proportional to the number of cells with potential for CH<sub>4</sub> production (Luton *et al.*, 2002; Steinberg & Regan, 2008) or consumption, because *mcrA* genes are also found in anaerobic CH<sub>4</sub> oxidizers (Raghoebarsing *et al.*, 2006; Beal *et al.*, 2009; Ettwig *et al.*, 2010).

In Siq surface sediment, the *mcrA* gene copy numbers were low but detectable, while *mcrA* copy numbers in Suk were below the limits of detection established for the assay at both sites. This pattern may at least partly explain the observed difference in CH<sub>4</sub> concentration between the two lakes and is a good approximation of relative differences between the lakes. In comparison with *mcrA* copy numbers found in a sample of active layer (permafrost) from the Canadian High Arctic (Yergeau *et al.*, 2010), the *mcrA* copy numbers detected in Siq11 were 1 to 2 orders of magnitude higher. Also, our results are quite comparable to two active layer samples from the Western Canadian Arctic, where *mcrA* copies g<sup>-1</sup> wet soil were between 10<sup>3</sup> and 10<sup>6</sup> (Frank-Fahle *et al.*, 2014), although our highest copy number was 1.86 × 10<sup>4</sup> *mcrA* copies g<sup>-1</sup> sediment in Siq.

Archaeal (in this case methanogen) biomass was corroborated by the detection of archaeol in the lake sediments (Mccartney *et al.*, 2013). Archaeol is an isoprenoid membrane lipid produced by archaea that has been attributed in freshwater sediments and peats to methanogenic archaea, (Pancost *et al.*, 2011). The presence of archaeol may reflect active shallow sedimentary archaea (Parkes *et al.*, 2007) or preserved dead microbial biomass (Pancost *et al.*, 2011; Bischoff *et al.*, 2013). In either case, not only was the concentration of archaeol much higher in Siq than in SukB and SukS, but it also tracked the trends of *mcrA* copy numbers per gram of sediment, amounts of TOC, and CH<sub>4</sub> concentrations observed in the depth profile of Siq, supporting the use of this compound as a proxy for methanogenic archaea in lacustrine environments. Compared to the concentrations of archaeol detected in an area of continuous permafrost in Siberia (Bischoff *et al.*, 2013), where CH<sub>4</sub> has been measured *in situ* and in incubations at 10 °C (Table S1), archaeol concentrations detected in the upper intervals of Siq were three orders of magnitude higher, and the concentrations detected in Suk were within the range of concentrations or slightly higher.

Archaeol abundance was also normalized to the C<sub>31</sub> *n*-alkane abundance, a lipid likely to derive primarily from diagenesis of land plant leaf waxes, to correct for terrigenous inputs, and to serve as a means of assessing which lake had the highest *in situ* archaeol production. Archaeol-to-*n*-C<sub>31</sub> ratio was consistently higher in Siq and SukB

than in the SukS site, indicating higher contributions from lake sedimentary archaea, above baseline values transported in by soil lipid inputs.

#### Amount of organic matter, sources, and its relevance to CH<sub>4</sub> production

Within and among the studied thermokarst lakes, organic matter content and composition were heterogeneous. Unlike Siberian permafrost where the main source of organic matter is from the Pleistocene (Zimov *et al.*, 1997), lacustrine sedimentary organic matter in these lakes appears to have a contribution from ongoing *in situ* primary production, as observed in other lakes of the North Slope of Alaska (Bretz & Whalen, 2014). Although ubiquitous in the environment and of moderately low source specificity, *n*-alkane chain length has been shown to differ between vascular plant waxes (typically odd carbon number *n*-alkanes greater than C<sub>22</sub>; Killops & Killops, 2005) and microbial lipids (approximately C<sub>16</sub>–C<sub>24</sub>; reviewed in Meyers & Ishiwatari, 1993). Additionally, *n*-alkane chain length may reflect the proportion of submerged vs. emergent or terrigenous macrophytes, in which submerged macrophytes produce larger proportions of shorter (C<sub>23</sub>, C<sub>25</sub>) *n*-alkanes (Ficken *et al.*, 2000).

The dominance of intermediate chain length *n*-alkanes in Siq sediments indicated a substantial organic contribution from a mixture of aquatic microbial lipids (bacteria) and algae, and terrestrial plants and soils. Siq *P*<sub>aq</sub> values were consistent with a source from submerged macrophytes or microbial primary producers. Sterane-to-hopane ratios reflected the relative contributions of plants and algae vs. hopanoid-producing bacteria, with a larger proportion of eukaryotic material present in the bound fraction.

Suk organic matter showed a greater contribution from allochthonous, perhaps more resistant or reworked organic matter. Free hydrocarbons in SukS were dominated by terrigenous leaf waxes (larger amounts of long-chain *n*-alkanes with high CPI; Tables S2 and S3) and trace amounts of mature diastereoisomers of steranes and hopanes, indicating a small contribution from petroleum at this site. *P*<sub>aq</sub> values for the free *n*-alkanes in SukS sediments also reflected supply from terrigenous plants including bryophytes (e.g., *Pogonatum* sp. which produces low amounts of C<sub>25</sub>, C<sub>27</sub>, and C<sub>23</sub> *n*-alkanes; Haas, 1982), while the longer chain *n*-alkanes more likely derived from graminoids (e.g., *Arctophila fulva*, *Carex* spp., and *Eriophorum* spp. which produce predominantly C<sub>27</sub>, C<sub>31</sub>, and C<sub>29</sub> *n*-alkanes; Oros *et al.*, 2006; Ronkainen *et al.*, 2013). However, high sterane-to-hopane ratios (with C<sub>29</sub> steranes the most abundant) and elevated short-chain *n*-alkanes in the kerogen-bound hydrocarbons showed significant inputs of likely microbially derived *n*-alkanes. These findings from bound

organics from the kerogen phase most likely reflect additional, though proportionately less abundant inputs from C<sub>29</sub> steroid-producing algae or macrophytes (e.g., chlorophytes) in comparison with Siq.

Microbial CH<sub>4</sub> production rates in lake sediments can be controlled by the amount of dissolved or total organic carbon (Kelly & Chynoweth, 1981; Bergman *et al.*, 2000; Avery *et al.*, 2003; Liu *et al.*, 2011). In this study, organic matter composition and proxies for methanogen abundance also seemed to influence CH<sub>4</sub> production. For instance, the maximum amount of organic carbon observed in SukB sediments was comparable to that of the methanogenic zone in Siq; however, organic carbon in Suk was more recalcitrant than in Siq, and archaeol concentrations in Suk were much lower, perhaps explaining the low to non-existent CH<sub>4</sub> production in this lake. Moreover, in Siq sediments, TOC in excess of 10 wt. % extended to 42 cm, but archaeol concentrations diminished below ~22 cm, suggesting the depletion of readily available fermentation products with depth as well. TOC content may not be used as sole predictor of short-term CH<sub>4</sub> production in these lakes; the lability of sedimentary organic matter influences the amount and composition of substrates ultimately available for methanogenesis.

#### Implications for CH<sub>4</sub> production from permafrost in the North American Arctic

In comparison with permafrost samples from other arctic environments, the amount of CH<sub>4</sub> produced in incubations of Siq and SukB sediments was 2–3 orders of magnitude higher, while the amount of CH<sub>4</sub> accumulated in the sediments of the lakes was within the range of CH<sub>4</sub> concentrations detected in other arctic locations (Table S1). Note that we have not taken seasonal or interannual variation in this study (beyond dissolved CH<sub>4</sub> concentrations and the carbon isotopes), which may introduce some degree of uncertainty upon our observations. Assuming an average porosity of  $0.28 \pm 0.07$ , an average headspace volume of  $0.009 \pm 0.001$  L, and an average sediment volume of  $0.003 \pm 0.001$  L, CH<sub>4</sub> concentrations detected in Siq11 ranged between ~121.40 μM and ~4.89 mM. Conversely, CH<sub>4</sub> concentrations in SukB11 ranged between ~0.75 μM and ~5.80 μM, and CH<sub>4</sub> concentrations in SukS11 ranged between ~12.62 μM and ~405.12 μM. These concentrations are comparable to CH<sub>4</sub> concentrations detected 60 miles to the south in Qalluuraq Lake, which has active gas seeps, although the concentrations in the first ~30-cm sediments of Siq11 were ~2.5 × higher than in Qalluuraq Lake sediments (He *et al.*, 2012). Moreover, CH<sub>4</sub> concentrations in Siq exceeded the maximum CH<sub>4</sub> concentration detected in lake GTH 112 in the Arctic Foothills region by approximately an order of magnitude which displayed a similar

trend in the pore water CH<sub>4</sub> profile (Bretz & Whalen, 2014).

Our study demonstrated that methanogenic archaea present in Alaska's North Slope thermokarst lakes are able to use *in situ* substrates for methanogenesis in a temperature-dependent fashion and that the amount of CH<sub>4</sub> produced is proportional to the *mcrA* copy number, the concentration of archaeol, and the amount of labile organic matter in the sediments. These findings are particularly important when considering possible scenarios of climate change (Yvon-Durocher *et al.*, 2014). The effect of increasing the temperature by 8 °C (from 2 to 10 °C) on CH<sub>4</sub> production rates was substantial for Siq. Currently, the largest source of CH<sub>4</sub> in this region of the North Slope of Alaska is the release of thermogenic CH<sub>4</sub> (Walter Anthony *et al.*, 2012). In scenarios of warming climate, our data lead us to contend that biological CH<sub>4</sub> production may play a larger role in CH<sub>4</sub> emissions in the future, although here, we have not considered CH<sub>4</sub> sinks (e.g., methanotrophy), which will also likely respond in parallel with temperature (Lofton *et al.*, 2014).

A point of caution is that this study focused on the interior of the lakes, although it is possible CH<sub>4</sub> production varies throughout the lakes and may be strongest at organic-rich thermokarst lake margins. Therefore, future estimates of CH<sub>4</sub> emissions should comprise spatial characterization and include the organic-rich shelf area, to be an adequate predictor of CH<sub>4</sub> release from Alaskan thermokarst lakes. CH<sub>4</sub> emission estimates would also benefit from including annual components of the production cycle to account for the impact of temperature shifts. With these cautions in mind, this study constitutes an important first step in determining the contribution of biogenic CH<sub>4</sub> to CH<sub>4</sub> budgets in the changing Alaskan arctic environment in proximal, yet contrasting thermokarst lake ecosystems.

#### ACKNOWLEDGMENTS

We especially thank A. Klesh, J. Leichty, and P. Santibañez, for assistance in the field; K. Walter Anthony for sharing her observations about the study area; and Frank Löffler for analyses of pore waters in the University of Tennessee. We are very grateful to N. Riedinger, J. Memmott, G. Miller, E. Ulrich, M. Miller, G. Trubl, J. Dodsworth, B. Hedlund, and J. Qualls for invaluable technical support. Likewise, we appreciate the efforts of the Barrow Arctic Science Consortium (BASC) and the UMIAQ Corporation in Barrow, AK, for providing logistical support and insight into the local region. Special thanks to the anonymous reviewers of the manuscript and to Life Technologies for use of the Applied Biosystems 7500 Fast system to conduct qPCR. PMC was supported in part by the Division of Earth and Ecosystem Sciences, DRI. Funding for ABM was provided in part by NSF IGERT Program in Geobio-

logical Systems (DGE 0654336). KPH and DB acknowledge support through the Jet Propulsion Laboratory (JPL), California Institute of Technology, under contract with the National Aeronautics and Space Administration (NASA). Financial support for this work was provided in part by the NASA Astrobiology Institute, Astrobiology of Icy Worlds program at JPL, and a NASA Astrobiology Science and Technology for Exploring Planets (ASTEP) award (Project Narvak, NNN13D036T). Support from these programs is gratefully acknowledged.

## REFERENCES

- Avery GB, Shannon RD, White JR, Martens CS, Alperin MJ (2003) Controls on methane production in a tidal freshwater estuary and a peatland: methane production via acetate fermentation and CO<sub>2</sub> reduction. *Biogeochemistry* **62**, 19–37.
- Baker MA, Vervier P (2004) Hydrological variability, organic matter supply and denitrification in the Garonne River ecosystem. *Freshwater Biology* **49**, 181–190.
- Banihani Q, Sierra-Alvarez R, Field J (2009) Nitrate and nitrite inhibition of methanogenesis during denitrification in granular biofilms and digested domestic sludges. *Biodegradation* **20**, 801–812.
- Beal EJ, House CH, Orphan VJ (2009) Manganese- and iron-dependent marine methane oxidation. *Science* **325**, 184–187.
- Bergman I, Klarqvist M, Nilsson M (2000) Seasonal variation in rates of methane production from peat of various botanical origins: effects of temperature and substrate quality. *FEMS Microbiology Ecology* **33**, 181–189.
- Bischoff J, Mangelsdorf K, Gattinger A, Schlöter M, Kurchatova AN, Herzschuh U, Wagner D (2013) Response of methanogenic archaea to Late Pleistocene and Holocene climate changes in the Siberian Arctic. *Global Biogeochemical Cycles* **27**, 305–317.
- Boetius A, Damm E (1998) Benthic oxygen uptake, hydrolytic potentials and microbial biomass at the arctic continental slope. *Deep-Sea Research Part I-Oceanographic Research Papers* **45**, 239–275.
- Bonilla S, Villeneuve V, Vincent WF (2005) Benthic and planktonic algal communities in a High Arctic lake: pigment structure and contrasting responses to nutrient enrichment. *Journal of Phycology* **41**, 1120–1130.
- Bretz KA, Whalen SC (2014) Methane cycling dynamics in sediments of Alaskan Arctic Foothill lakes. *Inland Waters* **4**, 65–78.
- Broecker WS, Peng TH (1974) Gas-exchange rates between air and sea. *Tellus* **26**, 21–35.
- Carson CE, Hussey KM (1962) The oriented lakes of Arctic Alaska. *The Journal of Geology* **70**, 417–439.
- Chong S, Liu Y, Cummins M, Valentine D, Boone D (2002) *Methanogenium marinum* sp. nov., a H<sub>2</sub>-using methanogen from Skan Bay, Alaska, and kinetics of H<sub>2</sub> utilization. *Antonie van Leeuwenhoek* **81**, 263–270.
- Colwell FS, Boyd S, Delwiche ME, Reed DW, Phelps TJ, Newby DT (2008) Estimates of biogenic methane production rates in deep marine sediments at Hydrate Ridge, Cascadia margin. *Applied and Environmental Microbiology* **74**, 3444–3452.
- Conrad R, Schutz H (1988) Methods for studying methanogenic bacteria and methanogenic activities in aquatic environments. In *Methods in Aquatic Bacteriology* (ed. Austin B). Wiley, Chichester, UK, pp. 301–343.
- Davidson EA, Janssens IA (2006) Temperature sensitivity of soil carbon decomposition and feedbacks to climate change. *Nature* **440**, 165–173.
- D'hondt SL, Jørgensen BB, Miller DJ (2003) Chapter 5. Explanatory notes. In: *Proceedings of the Ocean Drilling Program*, pp. 102.
- Duc NT, Crill P, Bastviken D (2010) Implications of temperature and sediment characteristics on methane formation and oxidation in lake sediments. *Biogeochemistry* **100**, 185–196.
- Ettwig KF, Butler MK, Le Paslier D, Pelletier E, Mangenot S, Kuypers MMM, Schreiber F, Dutilh BE, Zedelius J, De Beer D, Gloerich J, Wessels H, Van Alen T, Luesken F, Wu ML, Van De Pas-Schoonen KT, Den Camp H, Janssen-Megens EM, Francoijs KJ, Stunnenberg H, Weissenbach J, Jetten MSM, Strous M (2010) Nitrite-driven anaerobic methane oxidation by oxygenic bacteria. *Nature* **464**, 543–548.
- Ficken KJ, Li B, Swain DL, Eglinton G (2000) An *n*-alkane proxy for the sedimentary input of submerged/floating freshwater aquatic macrophytes. *Organic Geochemistry* **31**, 745–749.
- Frank-Fahle BA, Yergeau E, Greer CW, Lantuit H, Wagner D (2014) Microbial functional potential and community composition in permafrost-affected soils of the NW Canadian Arctic. *PLoS One* **9**, e84761.
- Freitag TE, Prosser JI (2009) Correlation of methane production and functional gene transcriptional activity in a peat soil. *Applied and Environmental Microbiology* **75**, 6679–6687.
- French HM (1976) *The Periglacial Environment*. Longman Inc, New York.
- Frohn RC, Hinkel KM, Eisner WR (2005) Satellite remote sensing classification of thaw lakes and drained thaw lake basins on the North Slope of Alaska. *Remote Sensing of Environment* **97**, 116–126.
- Glenn RK, Allen WW (1992) Geology, reservoir engineering and methane hydrate potential of the Walakpa Gas Field, North Slope, Alaska. In: Final technical report (under grant DE-FG21-91MC28131) submitted to the U.S. Department of Energy. North Slope Borough, Barrow, AK, pp. 1–26.
- Haas K (1982) Surface wax of *Andreaea* and *Pogonatum* species. *Phytochemistry* **21**, 657–659.
- He R, Wooller MJ, Pohlman JW, Quensen J, Tiedje JM, Leigh MB (2012) Diversity of active aerobic methanotrophs along depth profiles of arctic and subarctic lake water column and sediments. *ISME Journal* **6**, 1937–1948.
- Hecky RE, Hesslein RH (1995) Contributions of benthic algae to lake food webs as revealed by stable isotope analysis. *Journal of the North American Benthological Society* **14**, 631–653.
- Hinkel KM, Eisner WR, Bockheim JG, Nelson FE, Peterson KM, Dai XY (2003) Spatial extent, age, and carbon stocks in drained thaw lake basins on the Barrow Peninsula, Alaska. *Arctic Antarctic and Alpine Research* **35**, 291–300.
- Hochachka PW, Somero GN (1973) *Strategies of Biochemical Adaptation*. Saunders, Philadelphia.
- Hoehler T, Alperin MJ (2014) Methane minimalism. *Nature* **507**, 436–437.
- Houseknecht DW, Bird KJ, Schuenemeyer JH, Attanasi ED, Garrity CP, Schenk CJ, Charpentier RR, Pollastro RM, Cook TA, Klett TR (2010) 2010 updated assessment of undiscovered oil and gas resources of the National Petroleum Reserve in Alaska (NPR). In: U.S. Geological Survey Fact Sheet 2010, pp. 4.
- Howard HH, Prescott GW (1973) Seasonal variation of chemical parameters in Alaskan tundra lakes. *American Midland Naturalist* **90**, 154–164.
- Hussey KM, Michelson RW (1966) Tundra relief features near Point Barrow Alaska. *Arctic* **19**, 162.

- Johnson LT, Royer TV, Edgerton JM, Leff LG (2012) Manipulation of the dissolved organic carbon pool in an agricultural stream: responses in microbial community structure, denitrification, and assimilatory nitrogen uptake. *Ecosystems* **15**, 1027–1038.
- Jorgenson MT, Shur Y (2007) Evolution of lakes and basins in northern Alaska and discussion of the thaw lake cycle. *Journal of Geophysical Research* **112**, 1–12.
- Jorgenson T, Yoshikawa K, Kanevskiy M, Shur Y, Romanovsky VE, Marchenko S, Grosse G, Brown J, Jones B (2008) *Permafrost Characteristics of Alaska*, Institute of Northern Engineering, University of Alaska, Fairbanks.
- Judd AG (2000) Geological sources of methane. In *Atmospheric Methane. Its Role in the Global Environment* (ed. Khalil MAK). Springer, New York, pp. 280–303.
- Kelly CA, Chynoweth DP (1981) The contributions of temperature and the input of organic-matter in controlling rates of sediment methanogenesis. *Limnology and Oceanography* **26**, 891–897.
- Kiene RP, Capone DG (1985) Degassing of pore water methane during sediment incubations. *Applied and Environmental Microbiology* **49**, 143–147.
- Killops SD, Killops VJ (2005) *Introduction to Organic Geochemistry*. Blackwell Publishing Ltd, Oxford.
- Kinnaman FS, Valentine DL, Tyler SC (2007) Carbon and hydrogen isotope fractionation associated with the aerobic microbial oxidation of methane, ethane, propane and butane. *Geochimica et Cosmochimica Acta* **71**, 271–283.
- Kittel TGF, Baker BB, Higgins JV, Hanev JC (2011) Climate vulnerability of ecosystems and landscapes on Alaska's North Slope. *Regional Environmental Change* **11**, S249–S264.
- Koch K, Knoblauch C, Wagner D (2009) Methanogenic community composition and anaerobic carbon turnover in submarine permafrost sediments of the Siberian Laptev Sea. *Environmental Microbiology* **11**, 657–668.
- Kokelj SV, Jorgenson MT (2013) Advances in thermokarst research. *Permafrost & Periglacial Processes* **24**, 108–119.
- Kvenvolden KA, Rogers BW (2005) Gaia's breath—global methane exhalations. *Marine and Petroleum Geology* **22**, 579–590.
- Ling F, Zhang T (2003) Numerical simulation of permafrost thermal regime and talik development under shallow thaw lakes on the Alaskan Arctic Coastal Plain. *Journal of Geophysical Research-Atmospheres* **108**, 1–11.
- Lipson DA, Raab TK, Gorla D, Zlamal J (2013) The contribution of Fe(III) and humic acid reduction to ecosystem respiration in drained thaw lake basins of the Arctic Coastal Plain. *Global Biogeochemical Cycles* **27**, 399–409.
- Liu DY, Ding WX, Jia ZJ, Cai ZC (2011) Relation between methanogenic archaea and methane production potential in selected natural wetland ecosystems across China. *Biogeosciences* **8**, 329–338.
- Liu Y, Yao T, Gleixner G, Claus P, Conrad R (2013) Methanogenic pathways,  $^{13}\text{C}$  isotope fractionation, and archaeal community composition in lake sediments and wetland soils on the Tibetan Plateau. *Journal of Geophysical Research: Biogeosciences* **118**, 650–664.
- Lofton DD, Whalen SC, Hershey AE (2014) Effect of temperature on methane dynamics and evaluation of methane oxidation kinetics in shallow arctic Alaskan lakes. *Hydrobiologia* **721**, 209–222.
- Love GD, Bowden SA, Jahnke LL, Snape CE, Campbell CN, Day JG, Summons RE (2005) A catalytic hydrolysis method for the rapid screening of microbial cultures for lipid biomarkers. *Organic Geochemistry* **36**, 63–82.
- Luton PE, Wayne JM, Sharp RJ, Riley PW (2002) The *mcrA* gene as an alternative to 16S rRNA in the phylogenetic analysis of methanogen populations in landfill. *Microbiology* **148**, 3521–3530.
- Maerki M, Muller B, Dinkel C, Wehrli B (2009) Mineralization pathways in lake sediments with different oxygen and organic carbon supply. *Limnology and Oceanography* **54**, 428–438.
- Mccartney CA, Bull ID, Waters SM, Dewhurst RJ (2013) Technical note: comparison of biomarker and molecular biological methods for estimating methanogen abundance. *Journal of Animal Science* **91**, 5724–5728.
- Meyers PA, Ishiwatari R (1993) Lacustrine organic geochemistry – an overview of indicators of organic-matter sources and diagenesis in lake-sediments. *Organic Geochemistry* **20**, 867–900.
- Mikan CJ, Schimel JP, Doyle AP (2002) Temperature controls of microbial respiration in arctic tundra soils above and below freezing. *Soil Biology & Biochemistry* **34**, 1785–1795.
- Negandhi K, Laurion I, Whitticar MJ, Galand PE, Xu X, Lovejoy C (2013) Small thaw ponds: an unaccounted source of methane in the Canadian High Arctic. *PLoS One* **8**, e78204.
- Nielsen LP, Christensen PB, Revsbech NP, Sorensen J (1990) Denitrification and oxygen respiration in biofilms studied with a microsensor for nitrous-oxide and oxygen. *Microbial Ecology* **19**, 63–72.
- Oechel WC, Hastings SJ, Vourlirts G, Jenkins M, Riechers G, Grulke N (1993) Recent change of arctic tundra ecosystems from a net carbon dioxide sink to a source. *Nature* **361**, 520–523.
- Oros DR, Abas MRB, Omar NYMJ, Rahman NA, Simoneit BRT (2006) Identification and emission factors of molecular tracers in organic aerosols from biomass burning: part 3. Grasses. *Applied Geochemistry* **21**, 919–940.
- Pancost RD, Mcclymont EL, Bingham EM, Roberts Z, Charman DJ, Hornibrook ERC, Blundell A, Chambers FM, Lim KLH, Evershed RP (2011) Archaeol as a methanogen biomarker in ombrotrophic bogs. *Organic Geochemistry* **42**, 1279–1287.
- Parkes RJ, Cragg BA, Banning N, Brock F, Webster G, Fry JC, Hornibrook E, Pancost RD, Kelly S, Knab N, Jorgensen BB, Rinna J, Weightman AJ (2007) Biogeochemistry and biodiversity of methane cycling in subsurface marine sediments (Skagerrak, Denmark). *Environmental Microbiology* **9**, 1146–1161.
- Parsekian AD, Grosse G, Walbrecker JO, Muller-Petke M, Keating K, Liu L, Jones BM, Knight R (2013) Detecting unfrozen sediments below thermokarst lakes with surface nuclear magnetic resonance. *Geophysical Research Letters* **40**, 535–540.
- Pedersen JA, Simpson MA, Bockheim JG, Kumar K (2011) Characterization of soil organic carbon in drained thaw-lake basins of Arctic Alaska using NMR and FTIR photoacoustic spectroscopy. *Organic Geochemistry* **42**, 947–954.
- Phelps AR, Peterson KM, Jeffries MO (1998) Methane efflux from high-latitude lakes during spring ice melt. *Journal of Geophysical Research* **103**, 29029.
- Quay PD, King SL, Lansdown JM, Wilbur DO (1988) Isotopic composition of methane released from wetlands: implications for the increase in atmospheric methane. *Global Biogeochemical Cycles* **2**, 385–397.
- Raghoebarsing AA, Pol A, Van De Pas-Schoonen KT, Smolders AJ, Ettwig KF, Rijpstra WI, Schouten S, Damste JS, Op Den Camp HJ, Jetten MS, Strous M (2006) A microbial consortium couples anaerobic methane oxidation to denitrification. *Nature* **440**, 918–921.
- Ramlal PS, Hesslein RH, Hecky RE, Fee EJ, Rudd JWM, Guildford SJ (1994) The organic-carbon budget of a shallow

- arctic tundra lake on the Tuktoyaktuk Peninsula, N. W. T. *Canada Biogeochemistry* **24**, 145–172.
- Rasmussen H, Jørgensen BB (1992) Microelectrode studies of seasonal oxygen-uptake in a coastal sediment – role of molecular diffusion. *Marine Ecology Progress Series* **81**, 289–303.
- Repenning CA (1983) New evidence for the age of the Gubik Formation Alaskan North Slope. *Quaternary Research* **19**, 356–372.
- Revsbech NP (1989) An oxygen microsensor with a guard cathode. *Limnology and Oceanography* **34**, 474–478.
- Riedinger N, Brunner B, Lin YS, Voßmeyer A, Ferdelman TG, Jørgensen BB (2010) Methane at the sediment–water transition in Black Sea sediments. *Chemical Geology* **274**, 29–37.
- Ronkainen T, Mcclymont EL, Välranta M, Tuittila E-S (2013) The *n*-alkane and sterol composition of living fen plants as a potential tool for palaeoecological studies. *Organic Geochemistry* **59**, 1–9.
- Schuur EAG, Vogel JG, Crummer KG, Lee H, Sickman JO, Osterkamp TE (2009) The effect of permafrost thaw on old carbon release and net carbon exchange from tundra. *Nature* **459**, 556–559.
- Seeborg-Elverfeldt J, Schlüter M, Feseker T, Kölling M (2005) Rhizon sampling of pore waters near the sediment/water interface of aquatic systems. *Limnology and oceanography, Methods* **3**, 361–371.
- Sellmann PV, Bown J, Lewellen RI, Mckim H, Merry C (1975) The classification and geomorphic implications of thaw lakes on the arctic coastal plain, Alaska, U.S. In: Army CRREL Research Report, pp. 21.
- Steinberg LM, Regan JM (2008) Phylogenetic comparison of the methanogenic communities from an acidic, oligotrophic fen and an anaerobic digester treating municipal wastewater sludge. *Applied and Environmental Microbiology* **74**, 6663–6671.
- Sweerts J, Bargilissen MJ, Cornelese AA, Cappenberg TE (1991) Oxygen-consuming processes at the profundal and littoral sediment water interface of a small meso-eutrophic lake (Lake Vechten, the Netherlands). *Limnology and Oceanography* **36**, 1124–1133.
- Tazaz AM, Bebout BM, Kelley CA, Poole J, Chanton JP (2013) Redefining the isotopic boundaries of biogenic methane: methane from endoevaporites. *Icarus* **224**, 268–275.
- Thien SJ (1979) A flow diagram for teaching texture-by-feel analysis. *Journal of Agronomic Education* **8**, 54–55.
- Wagner D, Gattinger A, Embacher A, Pfeiffer E-M, Schloter M, Lipski A (2007) Methanogenic activity and biomass in Holocene permafrost deposits of the Lena Delta, Siberian Arctic and its implication for the global methane budget. *Global Change Biology* **13**, 1089–1099.
- Walter Anthony KM, Anthony P, Grosse G, Chanton J (2012) Geologic methane seeps along boundaries of arctic permafrost thaw and melting glaciers. *Nature Geoscience* **5**, 419–426.
- Walter KM, Smith LC, Chapin FS 3rd (2007) Methane bubbling from northern lakes: present and future contributions to the global methane budget. *Philosophical Transactions. Series A, Mathematical, Physical, and Engineering Sciences* **365**, 1657–1676.
- Walter KM, Chanton JP, Chapin FS, Schuur EaG, Zimov SA (2008) Methane production and bubble emissions from arctic lakes: isotopic implications for source pathways and ages. *Journal of Geophysical Research*, **113**, 1–16.
- Whalen SC, Lofton DD, McGowan GE, Strohm A (2013) Microphytobenthos in shallow arctic lakes: fine-scale depth distribution of chlorophyll a, radiocarbon assimilation, irradiance, and dissolved O<sub>2</sub>. *Arctic, Antarctic, and Alpine Research* **45**, 285–295.
- Whiticar MJ (1999) Carbon and hydrogen isotope systematics of bacterial formation and oxidation of methane. *Chemical Geology* **161**, 291–314.
- Yergeau E, Hogues H, Whyte LG, Greer CW (2010) The functional potential of high Arctic permafrost revealed by metagenomic sequencing, qPCR and microarray analyses. *The ISME Journal* **4**, 1206–1214.
- Yvon-Durocher G, Allen AP, Bastviken D, Conrad R, Gudasz C, St-Pierre A, Thanh-Duc N, Del Giorgio PA (2014) Methane fluxes show consistent temperature dependence across microbial to ecosystem scales. *Nature* **507**, 488–491.
- Zhou S, Xu J, Yang G, Zhuang L (2014) Methanogenesis affected by the co-occurrence of iron(III) oxides and humic substances. *FEMS Microbiology Ecology* **88**, 107–120.
- Zimov SA, Voropaev YV, Semiletov IP, Davidov SP, Prosiannikov SF, Chapin FS, Chapin MC, Trumbore S, Tyler S (1997) North Siberian lakes: a methane source fueled by Pleistocene carbon. *Science* **277**, 800–802.

## SUPPORTING INFORMATION

Additional Supporting Information may be found in the online version of this article:

**Table S1.** CH<sub>4</sub> concentration and CH<sub>4</sub> production rates reported in the literature for arctic permafrost samples.

**Table S2.** Free hydrocarbon biomarker extracted from Siqluqaq and Sukok sediments.

**Table S3.** Lipid biomarker ratios from catalytic hydrolysis hydrocarbon products.

**Fig. S1.** Methane concentration and δ<sup>13</sup>C<sub>CH<sub>4</sub></sub> from all the cores collected for these analyses.